

Prevention of In droplets formation by HCl addition during metal organic vapor phase epitaxy of InN

Sang Won Kang, Hyun Jong Park, Yong Sun Won, Olga Kryliouk,^{a)} Tim Anderson, Dmitry Khokhlov,^{b)} and Timur Burbaev^{c)}

Department of Chemical Engineering, University of Florida, Gainesville, Florida 32611

(Received 25 January 2007; accepted 23 March 2007; published online 20 April 2007)

The low decomposition temperature of InN and relatively high thermal stability of NH₃ necessitate the use of a high NH₃/TMIn ratio to prevent In droplet formation on the surface. This work shows that the addition of Cl in the form of HCl (Cl/In molar ratio range of 0.3–1.4) to the growth chamber allows the growth of high quality InN films without the formation of a second In phase at a very low value of the N/In molar inlet ratio (2500). Photoluminescence spectra in the temperature range of 144 to 4.5 K showed a broad spectral band with a cutoff energy close to the reported minimum of the InN band gap energy (0.65 eV). © 2007 American Institute of Physics.

[DOI: 10.1063/1.2730582]

Until recently, interest in indium nitride (InN) was mainly derived from its role as a dilute component for enhancing emission efficiency of Ga_xIn_{1-x}N and Al_xIn_{1-x}N active layers in optoelectronic devices.^{1–5} Although pure InN is much less studied than GaN or AlN, significant differences in the measured optical properties have generated intense interest. Specifically, the band gap energy of wurtzite InN crystals, although still a subject of research, has been reported in the range of 0.65 to 0.9 eV.^{6–9} These values are considerably lower than the previously accepted value of 1.9 eV,¹⁰ suggesting applications for InN such as solar cells and infrared laser diodes.

The growth of InN films must overcome several challenges. The high N₂ equilibrium partial pressure over InN (Refs. 11 and 12) requires either a low growth temperature or high and reactive nitrogen over pressure. For deposition by metal organic vapor phase epitaxy (MOVPE), this translates into a growth temperature typically <650 °C and high N/In ratio (e.g., NH₃ to TMIn ratio >10⁴ at 650 °C) (Ref. 9) to avoid In liquid deposition during growth. The high N/In ratio is required since the homogeneous decomposition rate of NH₃ is low at 650 °C. At this condition it is estimated that less than 0.01 mol % of the inlet ammonia reacts with the In source, rendering the process extremely inefficient in NH₃ usage. The formation of liquid In droplets during growth is obviously undesirable because of its impact on the surface morphology and because it fixes the In chemical potential and thus the intrinsic equilibrium point defect structure of the grown InN. The growth of InN for device applications will require control of point defect concentrations (e.g., *p*-type doping, optical properties) and thus the ability to control the film N/In ratio, and specifically to increase it above that typically produced by MOVPE. Increasing the NH₃ partial pressure not only increases the reactive nitrogen but also decreases the In through reaction with hydrogen produced by ammonia decomposition.^{13,14} This then lowers the growth rate. In addition to growing at high ammonia partial pressure, the generation of reactive nitrogen radicals by both plasma-assisted^{15,16} and ArF excimer laser assisted MOVPE

(Ref. 17) has been demonstrated to avoid In droplet formation.

In this letter a simple approach to adjust the stoichiometry of InN is studied. The intentional addition of HCl to the growth chamber should form volatile indium chlorides [InCl (*T*_{bp}=450 °C) and InCl₃ (*T*_{sublimation}=500 °C)] to lower the In chemical potential. A series of films was grown at various HCl inlet partial pressures to test the feasibility of this approach in controlling In droplet formation and subsequently InN stoichiometry.

A simple equilibrium analysis was first performed to better understand the effect of HCl addition on the deposition chemistry. Kumagai *et al.* reported equilibrium calculations of hydride VPE of InN using either InCl or InCl₃ as the precursor. It is not surprising that they suggested that the higher Cl/In precursor, InCl₃, is preferred for deposition of InN since the thermodynamic driving force for the formation of InN is higher.^{18,19} Hydrogen, as derived from either decomposition of NH₃ or the carrier gas, decreases the driving force. Their results agree with the experimental observation that the growth of InN is higher with the use of InCl₃ versus InCl and when substituting inert N₂ for H₂ carrier. This analysis, however, only studied two values of the Cl/In inlet ratio (i.e., 1 and 3, depending on the In species used).

At typical InN deposition temperatures, the dominant InCl_x species is InCl. The effect of adding HCl to the reactor can be seen by comparing the Gibbs energy of the etching reactions for liquid In and solid InN to produce InCl and H₂ in addition to N₂ in the InN case. The standard ΔG_r° values for these two reactions were calculated using the ThermoCalc database SUB94 (Ref. 20) and plotted as a function of temperature in Fig. 1. It is clear that HCl attack of pure indium metal is preferred over reaction with InN and the large negative ΔG_r° at typical growth temperature should yield a significant reaction extent. It is also noted that ΔG_r° for etching InN is zero at 900 K, suggesting that at higher growth temperature, the addition of HCl will produce significant decrease in InN growth rate and possibly no growth.

The hypothesis that the addition of Cl to the deposition system can prevent deposition of In droplets during MOVPE of InN was tested in a reactor that has both MOVPE and hydride VPE capability. By adjusting the HCl/TMIn inlet molar ratio to values of 1 and 3, hydride VPE using either

^{a)}Electronic mail: olgak@grove.ufl.edu

^{b)}Also at Physics Department, Moscow State University, Moscow 119992, Russia.

^{c)}Also at Lebedev Physical Institute, Moscow 119991, Russia.

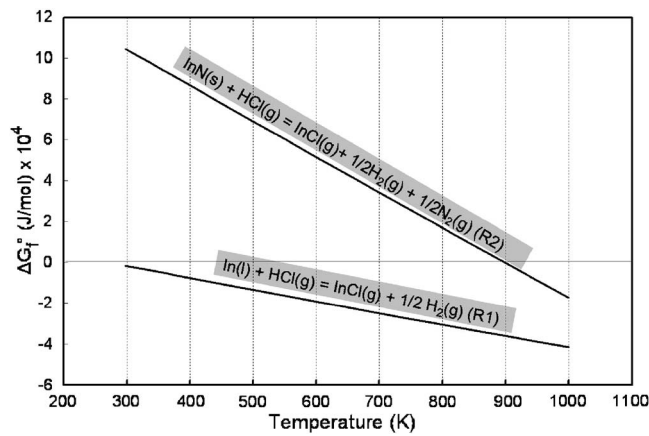


FIG. 1. Comparison of the standard Gibbs energy for etching reactions $\text{In}(l) + \text{HCl}(g) = \text{InCl}(g) + 1/2 \text{H}_2(g)$ and $\text{InN}(s) + \text{HCl}(g) = \text{InCl}(g) + 1/2 \text{H}_2(g) + 1/2 \text{N}_2(g)$.

InCl or InCl_3 was operational. A more complete description of this reactor is given elsewhere.²¹ InN was grown using TMIIn (TMIIn solution, Epichem), NH_3 (anhydrous grade 5, Matheson-Trigas), and HCl (10% HCl , 90% N_2 , Air Products) reactants on $c\text{-Al}_2\text{O}_3$ and $\text{GaN}/c\text{-Al}_2\text{O}_3$ ($5 \mu\text{m}$ thick GaN grown by MOVPE) substrates. For all films grown in this study, the operating pressure was 760 Torr and the growth temperature was 550°C , while the NH_3/TMIIn ratio was 2500. The total N_2 carrier gas flow rate was 4 slm (standard liters per minute) while the NH_3 and TMIIn flows were 1750 and 0.7 SCCM (SCCM denotes cubic centimeter per minute at STP), respectively. The HCl/TMIIn inlet molar ratio was varied in the range of 0–5 by changing the 10% HCl in N_2 gas flow rates from 0 to 35 SCCM.

Preliminary experiments indicated that MOVPE growth (i.e., no HCl feed) under these conditions gave two-phase In-InN growth. Two-phase deposition at this relatively low NH_3/TMIIn ratio is consistent with that previously reported.²² The x-ray diffraction pattern of a film grown on $\text{GaN}/c\text{-Al}_2\text{O}_3$ without HCl is shown in Fig. 2 bottom). The pattern clearly shows the presence of InN (002) and a strong In (101) peak. In contrast, the pattern for a film grown with a flow of 0.5 SCCM of HCl (HCl/TMIIn ratio=1.4) while

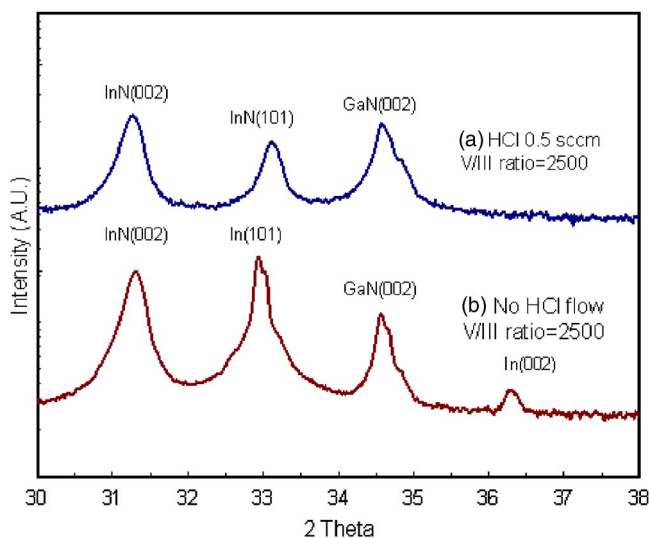


FIG. 2. X-ray diffraction patterns of InN grown on $\text{GaN}/\text{sapphire}$ (a) with HCl ($\text{HCl}/\text{TMIIn}=1.4$) and (b) without HCl flow at the base conditions $T=550^\circ\text{C}$ and $P=760$ Torr and N/In ratio=2500.

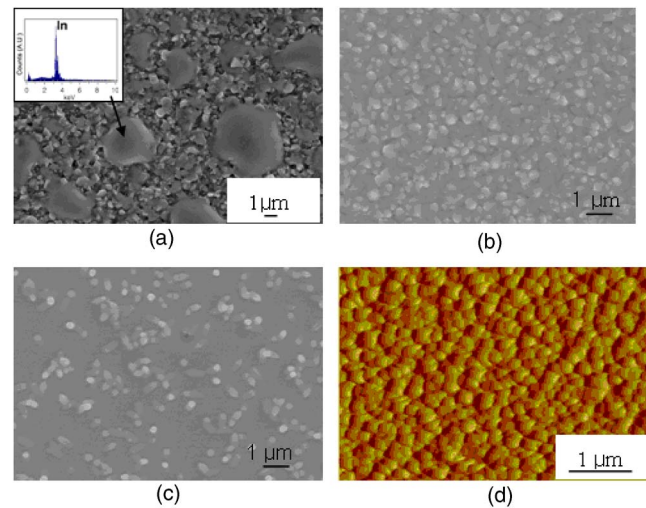


FIG. 3. SEM images of InN grown at base conditions on $\text{GaN}/c\text{-Al}_2\text{O}_3$ at various values of HCl/TMIIn molar ratio: (a) $\text{HCl}/\text{TMIIn}=0$ with insert displaying EDS In spectrum of In phase; (b) $\text{HCl}/\text{TMIIn}=1.0$; (c) $\text{HCl}/\text{TMIIn}=4.0$. (d) AFM image of InN grown at $\text{HCl}/\text{TMIIn}=1.0$.

maintaining the same NH_3/TMIIn ratio of 2500 shows no evidence for the formation of a pure In phase, as shown in Fig. 2 top spectrum). Some reduction in InN film growth rate ~ 1 to $\sim 0.8 \mu\text{m}/\text{h}$, however, was observed.

The surface morphology of the InN films grown at various values of HCl/TMIIn molar ratio was examined by scanning electron microscopy (SEM) and atomic force microscopy (AFM), while the composition was determined by Auger electron spectroscopy (AES) and energy dispersion spectroscopy (EDS). Only the $\text{GaN}/\text{Al}_2\text{O}_3$ substrates were examined in this study. Islands of pure solid In , presumably formed by solidification upon cooling of In droplets nucleated during growth, are clearly observed in the SEM image shown in Fig. 3(a) for the sample grown at the relatively low NH_3/TMIIn ratio (2500) of this study. An EDS analysis of one of the islands detected only In [see insert in Fig. 3(a)]. As shown in Fig. 3(a), the In surface feature size was variable ($3\text{--}5 \mu\text{m}$) for growth without HCl . This size variation suggests that during growth In droplet nucleation occurred at different times or they partially coalesced.

The SEM micrograph shown in Fig. 3(a) is contrasted to that shown in 3(b) for which HCl was added during film growth (HCl/TMIIn molar ratio=1). In this latter film, the InN is polycrystalline and In droplet formation was not evident. The rms roughness of the surface of the InN grown at HCl/TMIIn molar ratio=1 is 91.9 nm , as determined by AFM [Fig. 3(d)]. It is noted that In droplets did not nucleate on any films grown when HCl was added in the range of $0.3 \leq \text{HCl}/\text{TMIIn} \leq 5$. The observed surface morphologies of films grown with a HCl/TMIIn ratio in the range of 0.3–3.0 were similar to that shown in Fig. 3(b). As shown in the micrograph in Fig. 3(c), the surface was not completely covered at high HCl/TMIIn ratio=4.0, apparently because of the enhanced HCl etching of InN . Interestingly, for higher HCl/TMIIn molar ratio ≥ 5 , a sparse density of microrods was observed. AES did not detect chlorine to be within the detection limit ($\sim 0.1 \text{ at. } \%$) in the InN film even at the highest HCl/TMIIn ratio examined (5.0).

Figure 4(a) shows photoluminescence (PL) spectra collected at three measurement temperatures for an InN film grown on $\text{GaN}/\text{sapphire}$. The GaN film thickness was $5 \mu\text{m}$

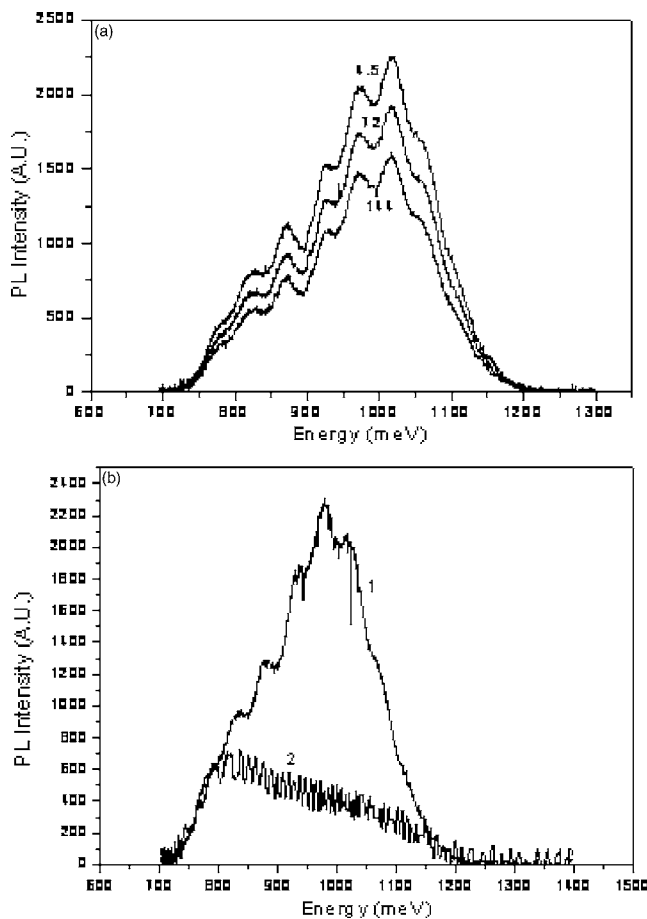


FIG. 4. (a) PL spectra measured at 4.2, 72, and 144 K, respectively (numbers near the curves are temperatures in K), for InN grown on GaN/sapphire at $T=550\text{ }^{\circ}\text{C}$ and $P=760\text{ Torr}$ and N/In ratio=2500 and $\text{HCl}/\text{TMin}=1$. (b) Room temperature PL spectra of InN grown at $T=550\text{ }^{\circ}\text{C}$ and $P=760\text{ Torr}$ and N/In ratio=2500 and $\text{HCl}/\text{TMin}=1$ on GaN/sapphire (1) and LT InN/sapphire (2).

and the $1\text{ }\mu\text{m}$ InN film was grown at the base conditions ($N/\text{In}=2500$, $T=550\text{ }^{\circ}\text{C}$) and HCl/TMin ratio=1. The PL occurs in a wide spectral band from 0.75 to 1.2 eV with a maximal PL intensity at about 1 eV. The spectral position of the PL maximum does not shift with temperature, while the PL intensity grows by a factor of about 1.5 upon lowering the measurement temperature from 144 to 4.5 K. Although not shown in this figure, there is little change in the PL spectra for samples grown at a HCl/TMin ratio in the range of 0.3–5.0.

One possible explanation for the wide energy band of the PL spectra is the formation of a graded $\text{In}_x\text{Ga}_{1-x}\text{N}$ interfacial region emanating from the InN/GaN interface. In this case, contribution of layers with different compositions would provide PL at different energies, thus forming a wide PL band. To determine if the GaN buffer layer affects the PL, films were grown on two different substrates, one with a GaN buffer layer and another with an InN buffer. Figure 4(b) compares room temperature PL spectra for two samples grown on *c* sapphire at the base conditions and HCl/TMin ratio =1.4 with either a GaN or a low-temperature InN buffer layer. The PL maximum in the GaN-free sample is strongly shifted to lower energy consistent with GaN incorporation in the InN film playing a significant role in shaping the PL spectra. The process of incorporating Ga into the InN could result from bulk diffusion or through initial etching of the GaN by HCl and reincorporation in the growing InN film. It

is important to note that the red cutoff energy of the PL band is close to the lowest reported gap value of InN (i.e., 0.65 eV).²³

In conclusion, the addition of Cl to the deposition zone was shown to be effective in reducing the In chemical potential. Simply adding a threshold level of HCl during growth led to the disappearance of In droplets that occurred at otherwise identical conditions. As suggested by a simple thermodynamic analysis and supported by experimental results, InN can be grown without the inclusion of a second phase at N/In ratio as low as 2500 by adding HCl in the HCl/TMin molar ratio range of 0.3–1.4 without chlorine incorporation. PL spectra of InN films show emission over a wide energy range with a lower edge close to the lowest reported value of 0.65 eV. Comparison of room temperature PL spectra for films grown with and without a GaN buffer layer on *c* sapphire gives results that are consistent with the formation of a $\text{Ga}_x\text{In}_{1-x}\text{N}$ interfacial layer on the GaN buffer layer.

Work at the University of Florida was supported by U.S. Army Grant No. 32051. Work at the Lebedev Physical Institute, Moscow, was partly supported by Programs of the RF Project Nos. 1923.2003.2 and 964/1989.

¹S. F. Chichibu, T. Azuhata, T. Sota, T. Mukai, and S. Nakamura, *J. Appl. Phys.* **88**, 5153 (2000).

²T. Onuma, A. Chakraborty, B. A. Haskell, S. Keller, S. P. DenBaars, J. S. Speck, S. Nakamura, U. K. Mishra, T. Sota, and S. F. Chichibu, *Appl. Phys. Lett.* **86**, 151918 (2005).

³S. Nakamura, M. Senoh, S. Nagahama, N. Iwasa, T. Matsushita, and T. Mukai, *Appl. Phys. Lett.* **76**, 22 (2000).

⁴F. Rizzi, P. R. Edwards, I. M. Watson, and R. W. Martin, *Superlattices Microstruct.* **40**, 369 (2006).

⁵T. Fujimori, H. Imai, A. Wakahara, H. Okada, A. Yoshida, T. Shibata, and M. Tanaka, *J. Cryst. Growth* **272**, 381 (2004).

⁶V. Y. Davydov, A. A. Klochikhin, R. P. Seisyan, V. V. Emtsev, S. V. Ivanov, F. Bechstedt, J. Furthmuller, H. Harima, A. V. Mudryi, J. Aderhold, O. Semchinova, and J. Graul, *Phys. Status Solidi B* **229**, R1 (2002).

⁷J. Wu, W. Walukiewicz, K. M. Yu, J. W. Ager III, E. E. Haller, H. Lu, W. J. Schaff, Y. Saito, and Y. Nanishi, *Appl. Phys. Lett.* **80**, 3967 (2002).

⁸J. Wu, W. Walukiewicz, W. Shan, K. M. Yu, J. W. Ager III, E. E. Haller, H. Lu, and W. J. Schaff, *Phys. Rev. B* **66**, 201403 (2002).

⁹T. Matsuoka, H. Okamoto, M. Nakao, H. Harima, and E. Kurimoto, *Appl. Phys. Lett.* **81**, 1246 (2002).

¹⁰T. L. Tansley and C. P. Foley, *J. Appl. Phys.* **59**, 3241 (1986).

¹¹O. Ambacher, J. Majewski, C. Miskys, A. Link, M. Hermann, M. Eickhoff, M. Stutzmann, F. Bernardini, V. Fiorentini, V. Tilak, B. Schaff, and L. F. Eastman, *J. Phys.: Condens. Matter* **14**, 3399 (2002).

¹²B. Onderka, J. Unland, and R. Schmid-Fetzer, *J. Mater. Res.* **17**, 3065 (2002).

¹³T. Matsuoka, H. Tanaka, T. Sasaki, and A. Katsui, *Proceedings of the 16th International Symposium on GaAs and Related Compounds*, Karuizawa, Japan, 25–29 September 1989 (IOP, Bristol, 1990), p. 141.

¹⁴A. Koukitu, T. Taki, N. Takahashi, and H. Seki, *J. Cryst. Growth* **197**, 99 (1999).

¹⁵A. Wakahara and A. Yoshida, *Appl. Phys. Lett.* **54**, 709 (1989).

¹⁶A. Wakahara, T. Tsuchiya, and A. Yoshida, *J. Cryst. Growth* **99**, 385 (1990).

¹⁷A. G. Bhuiyan, T. Tanaka, K. Kasashima, A. Hashimoto, and A. Yamamoto, *Jpn. J. Appl. Phys., Part 1* **42**, 7284 (2003).

¹⁸Y. Kumagai, K. Takemoto, A. Koukitu, and H. Seki, *J. Cryst. Growth* **222**, 118 (2001).

¹⁹A. Koukitu and Y. Kumagai, *J. Phys.: Condens. Matter* **13**, 6907 (2001).

²⁰B. Sundman, B. Janson, and J. O. Anderson, *CALPHAD: Comput. Coupling Phase Diagrams Thermochem.* **9**, 153 (1985).

²¹O. Kryliouk, M. Reed, T. Dann, T. Anderson, and B. Chai, *Mater. Sci. Eng., B* **59**, 6 (1999).

²²T. Matsuoka, *Superlattices Microstruct.* **37**, 19 (2005).

²³K. S. A. Butcher and T. L. Tansley, *Superlattices Microstruct.* **38**, 19 (2005).